Solution Structure, Dimerization, and Dynamics of a Lipophilic α/3₁₀-Helical, Cα-Methylated Peptide. Implications for Folding of Membrane Proteins

Alexander Dehner,[†] Eckart Planker,[†] Gerd Gemmecker,[†] Quirinus B. Broxterman,[‡] William Bisson,[‡] Fernando Formaggio,[§] Marco Crisma,[§] Claudio Toniolo,[§] and Horst Kessler*,[†]

Contribution from the Institut für Organische Chemie und Biochemie, Technische Universität München, Lichtenbergstrasse 4, 85747, Garching, Germany, DSM Research, Organic Chemistry and Biotechnology Section, P.O. Box 18, 6160 MD Geleen, The Netherlands, Biopolymer Research Center, CNR, Department of Organic Chemistry, University of Padova, Via Marzolo 1, 35131 Padova, Italy

Received March 9, 2001. Revised Manuscript Received May 2, 2001

Abstract: The solution structure and the dimerization behavior of the lipophilic, highly Cα-methylated model peptide, *m*BrBz-Iva[1]-Val[2]-Iva[3]-(αMe)Val[4]-(αMe)Phe[5]-(αMe)Val[6]-Iva[7]-NHMe, was studied by NMR spectroscopy and molecular dynamics simulations. The conformational analysis resulted in a right-handed 3₁₀/α-helical equilibrium fast on the NMR time scale with a slight preference for the α-helical conformation. The NOESY spectrum showed intermolecular NOEs due to an aggregation of the heptapeptide. In addition, temperature-dependent diffusion measurements were performed to calculate the hydrodynamic radius. All these findings are consistent with an antiparallel side-by-side dimerization. The structure of the dimeric peptide was calculated with a simulated annealing strategy. The lipophilic dimer is held together by favorable van der Waals interactions in the sense of a bulge fitting into a groove. The flexibility of the helical conformations concerning an α/3₁₀-helical equilibrium is shown in a 3 ns molecular dynamics simulation of the resulting dimeric structure. Both overall helical structures of each monomer and the antiparallel mode of dimerization are stable. However, transitions were seen of several residues from a 3₁₀-helical into an α-helical conformation and vice versa. Hence, this peptide represents a good model in which two often-discussed aspects of hierarchical transmembrane protein folding are present: $i \leftarrow i + 3$ and $i \leftarrow i + 4$ local H-bonding interactions cause a specific molecular shape which is then recognized as attractive by other surrounding structures.

Introduction

Theoretical and experimental work suggests that folding of helical membrane proteins can be considered as a two-stage process.[1−3] In a first step, hydrophobic helices are formed across the lipid membrane, stabilized by specific hydrogen bonding interactions. In a second step, the helical secondary structures interact to produce the native tertiary structure. These peptide helix−helix interactions are largely governed by van der Waals forces and shape complementarity.[4−6] NMR studies have shown that individual helical fragments of bacteriorhodopsin (BR) adopt their native-like conformation in membrane-mimicking media such as chloroform.[7] In addition, NMR dynamic studies have pointed to a flexibility of the helical part of (1−36)BR on the nano- and picosecond time scales, which could be attributed

to a local switching between 3₁₀-, α-, and π-helices and random coil conformations.[8]

Here we report an NMR and molecular dynamics study of the lipophilic heptapeptide *m*BrBz-Iva[1]-Val[2]-Iva[3]-(αMe)Val[4]-(αMe)-Phe[5]-(αMe)Val[6]-Iva[7]-NHMe [*m*BrBz, *meta*-bromobenzoyl; Iva, isovaline; (αMe)Val, Cα-methyl valine; (αMe)Phe, Cα-methyl phenylalanine; NHMe, methylamino], in which six of the seven Hα protons are substituted by methyl groups (Figure 1). It is well documented that peptides rich in Cα-methylated α-amino acids such as Aib (α-aminoisobutyric acid) or Iva have a tendency to adopt either the 3₁₀- or the α-helical conformation in the crystalline state[9−11] as well as in structure-supporting solvents.[12,13] It was the aim of this work to investigate the 3₁₀/α-helical equilibrium in chloroform solution, which mimics the lipophilic membrane core.

The geometry of a 3₁₀-helical hydrogen bond is less favorable than the α-helical geometry, although this effect is partly

* To whom correspondence should be addressed. Tel.: (+49) 89 289 13300. Fax: (+49) 89 289 13210. E-mail: Kessler@ch.tum.de.
† Technische Universität München.
‡ DSM Research.
§ University of Padova.

(1) Popot, J. L.; Engelman, D. M. *Biochemistry* **1990**, *29*, 4031−4037.
(2) Baldwin, R. L.; Rose, G. D. *Trends Biochem. Sci.* **1999**, *24*, 77−83.
(3) Baldwin, R. L.; Rose, G. D. *Trends Biochem. Sci.* **1999**, *24*, 26−33.
(4) MacKenzie, K. R.; Engelman, D. M. *Proc. Natl. Acad. Sci. U.S.A.* **1998**, *95*, 3583−3590.
(5) Petrache, H. I.; Grossfield, A.; MacKenzie, K. R.; Engelman, D. M.; Woolf, T. B. *J. Mol. Biol.* **2000**, *302*, 727−746.
(6) Russ, W. P.; Engelman, D. M. *J. Mol. Biol.* **2000**, *296*, 911−919.
(7) Pervushin, K. V.; Arseniev, A. S. *Bioorg. Khim.* **1995**, *21*, 83−111.

(8) Gratias, R.; Kessler, H. *J. Phys. Chem. B* **1998**, *102*, 2027−2031.
(9) Karle, I. L.; Balaram, P. *Biochemistry* **1990**, *29*, 6747−6756.
(10) Toniolo, C.; Benedetti, E. *Macromolecules* **1991**, *24*, 4004−4009.
(11) Toniolo, C.; Crisma, M.; Formaggio, F.; Cavicchioni, G.; Précigoux, G.; Aubry, A.; Kamphuis, J. *Biopolymers* **1993**, *33*, 1061−1072.
(12) Gratias, R.; Konat, R.; Crisma, M.; Kessler, H.; Valle, G.; Polese, A.; Formaggio, F.; Toniolo, C.; Broxterman, Q. B.; Kamphuis, J. *J. Am. Chem. Soc.* **1998**, *120*, 4763−4770.
(13) Formaggio, F.; Crisma, M.; Rossi, P.; Scrimin, P.; Kaptein, B.; Broxterman, Q. B.; Kamphuis, J.; Toniolo, C. *Chem. Eur. J.* **2000**, *6*, 4498−4504.
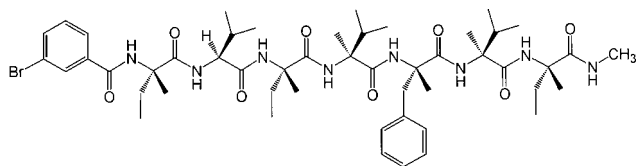
*m*BrBz-Iva[1]-Val[2]-Iva[3]-(αMe)Val[4]-(αMe)Phe[5]-(αMe)Val[6]-Iva[7]-NHMe

Figure 1. The highly Cα-methylated heptapeptide *m*BrBz-Iva[1]-Val[2]-Iva[3]-(αMe)Val[4]-(αMe)Phe[5]-(αMe)Val[6]-Iva[7]-NHMe studied in this work.

compensated for by a higher number of hydrogen bonds.[14,15] With increasing helical length, however, the α-helix, with its better hydrogen-bonding arrangement, becomes predominant. The 3₁₀-helix motif is found in 10% of all helical residues of globular proteins.[16] Most of the 3₁₀-helical stretches are fairly short; nevertheless, there are few cases in which the possible role of its occurrence could be addressed. For instance, a transition from an α- to a 3₁₀-helix is seen upon substrate binding to lactate dehydrogenase[17] or to mitochondrial aspartate aminotransferase.[18]

We show here that the N- and C-terminal blocked heptapeptide exhibits both a dynamic 3₁₀/α-helical equilibrium and a dimerization behavior due to favorable van der Waals interactions in the sense of shape complementarity such as a bulge fitting into a groove, and thus represents a good model system for protein folding in a lipophilic surrounding.

Materials and Methods

Synthesis and Characterization of Peptides. Melting points were determined with a Leitz (Wetzlar, Germany) model Laborlux 12 apparatus and are not corrected. Optical rotations were measured with a Perkin-Elmer (Norwalk, CT) model 241 polarimeter equipped with a Haake (Karlsruhe, Germany) model D thermostat. Thin-layer chromatography was performed on Merck (Darmstadt, Germany) Kieselgel 60F254 precoated plates with the following solvent systems: 1, chloroform/ethanol, 9:1; 2, 1-butanol/acetic acid/water, 3:1:1; 3, toluene/ethanol, 7:1. The chromatograms were examined using ultraviolet fluorescence or developed by chlorine/starch/potassium iodide or ninhydrin chromatic reaction as appropriate. All the compounds were obtained in a chromatographically homogeneous state. All of the synthetic intermediates and the final compound were also characterized by ¹H NMR.

For the large-scale production of the optically pure L-Iva, L-(αMe)-Val, and L-(αMe)Phe, we exploited an economically attractive, chemoenzymatic synthesis developed by DSM Research a few years ago.[19,20] It involves a combination of organic synthesis for the preparation of the racemic α-amino acids followed by the use of a broadly specific aminopeptidase to achieve optical resolution. The benzyloxycarbonyl (Z) Nα-protected, Cα-methylated α-amino acids[12,21] were activated by the acid fluoride method.[22] The Z group was removed by catalytic hydrogenation in methanol (MeOH) solution. The synthesis

and characterization of Z-Iva-(αMe)Val-(αMe)Phe-(αMe)Val-Iva-NHMe were already reported.[12]

Z-Val-Iva-(αMe)Val-(αMe)Phe-(αMe)Val-Iva-NHMe. This compound was obtained by reacting Z-Val-OH and H-Iva-(αMe)Val-(αMe)-Phe-(αMe)Val-Iva-NHMe in CH₂Cl₂ solution in the presence of 1-[3-(dimethylamino)propyl]-3-ethylcarbodiimide (EDC) hydrochloride, 1-hydroxy-7-aza-1,2,3-benzotriazole (HOAt),[23] and N-methylmorpholine (NMM). Yield 51%; mp 206−208 °C (from CHCl₃/petroleum ether); TLC 0.70 (**I**), 0.95 (**II**), 0.30 (**III**); [α]²⁰_D = 14.8° (*c* = 0.5, MeOH); IR (KBr) 3318, 1702, 1657, 1524 cm⁻¹.

Z-Iva-Val-Iva-(αMe)Val-(αMe)Phe-(αMe)Val-Iva-NHMe. This compound was prepared by reacting Z-Iva-F[12] and H-Val-Iva-(αMe)-Val-(αMe)Phe-(αMe)Val-Iva-NHMe (the latter obtained by catalytic hydrogenation of the corresponding Z-derivative) in CH₂Cl₂ solution in the presence of NMM. Yield 60%; mp 249−250 °C (from ethyl acetate/petroleum ether); TLC 0.65 (**I**), 0.90 (**II**), 0.30 (**III**); [α]²⁰_D = 12.4° (*c* = 0.5, MeOH); IR (KBr) 3312, 1696, 1656, 1526 cm⁻¹.

***m*BrBz-Iva-Val-Iva-(αMe)Val-(αMe)Phe-(αMe)Val-Iva-NHMe.** This compound was synthesized by reacting mBrBz-OAt[12] and H-Iva-Val-Iva-(αMe)Val-(αMe)Phe-(αMe)Val-Iva-NHMe (the latter obtained by catalytic hydrogenation of the corresponding Z-derivative) in a 9:1 CH₂Cl₂/CH₃CN solution in the presence of NMM. Yield 74%; mp 270−271 °C (from CH₂Cl₂/petroleum ether); TLC 0.60 (**I**), 0.95 (**II**), 0.20 (**III**); [α]²⁰_D = 17.0° (*c* = 0.2, MeOH); IR (KBr) 3315, 1654, 1526 cm⁻¹.

Nuclear Magnetic Resonance Measurements. A 6 mg sample of the heptapeptide (MW = 997.1) was dissolved at room temperature in 0.5 mL of CDCl₃ (*c* = 12 mmol/L). The solution was evacuated and fused in a 0.5 mm NMR tube to remove residual oxygen. The NMR measurements were performed on a Bruker (Rheinstetten, Germany) DMX 600 instrument (*B*₀ = 14.1 T). Processing and evaluation of the experimental data were carried out on an O2 workstation using XWinNMR Version 2.6 (Bruker). The optimal measuring conditions were found from a series of 1D proton spectra, which were recorded in the temperature range of 270−300 K. With the exception of the temperature-dependent diffusion measurements, all spectra were performed at 273 K, due to superior signal dispersion and to stabilize the proposed helical structure. At this temperature, however, the heptapeptide precipitated significantly so that its concentration in the saturated CDCl₃ solution was below 12 mmol/L. The ¹H spectra were recorded with 16 scans, a sweep width of 6009.62 Hz, a digital resolution of 16 384 real data points, and a relaxation delay of 1.0 s. The NOESY[24] spectrum was recorded with a spoil gradient during the mixing time (τ_m = 100 ms), with a sweep width of 6009.62 Hz in both dimensions, 512 real data points in F1 and 4096 real data points in F2, 48 scans per increment, and a relaxation delay of 1.0 s. For the data processing in F1, the data were zero-filled to 2048 data points, and a complex linear prediction was performed using 32 coefficients. Subsequently, in both dimensions a baseline correction was applied, and a squared sine bell function shifted by π/2 was used for apodization. The DQF−COSY[25] spectrum was recorded with 8 scans, sweep width 6009.62 Hz in both dimensions, 512 points in F1 and 4096 data points in F2, and a relaxation delay of 3.0 s. For the processing in F1, data were zero-filled to 2048 data points and to 8196 data points in F2. A subsequent baseline correction was applied in both dimensions. The TOCSY[26] spectrum was recorded with 8 scans, with a sweep width of 6009.62 Hz in both dimensions and a digital resolution of 512 in F1 and 4096 data points in F2 using a DIPSI[27] spin-lock mixing sequence with τ_m = 80 ms. For the data processing, F1 was zero-filled to 1024 real data points and F2 to 2048 real data points. A subsequent baseline correction was applied in both dimensions and a squared sine bell

(14) Toniolo, C.; Benedetti, E. *Trends Biochem. Sci.* **1991**, *16*, 350−353.

(15) Bolin, K. A.; Millhauser, G. L. *Acc. Chem. Res.* **1999**, *32*, 1027−1033.

(16) Barlow, D. J.; Thornton, J. M. *J. Mol. Biol.* **1988**, *201*, 601−619.

(17) Gerstein, M. C. *J. Mol. Biol.* **1991**, *220*, 133−149.

(18) McPhalen, C. A.; Vincent, M. G.; Picot, D.; Jansonius, J. N. *J. Mol. Biol.* **1992**, *227*, 197−213.

(19) Kruizinga, W. H.; Bolster, J.; Kellogg, R. M.; Kamphuis, J.; Boesten, W. H. J.; Meijer, E. M.; Schoemaker, H. E. *J. Org. Chem.* **1988**, *53*, 1826−1827.

(20) Kaptein, B.; Boesten, W. H. J.; Broxterman, Q. B.; Peters, P. J. H.; Schoemaker, H. E.; Kamphuis, J. *Tetrahedron: Asymmetry* **1993**, *4*, 1113−1116.

(21) Polese, A.; Formaggio, F.; Crisma, M.; Valle, G.; Toniolo, C.; Bonora, G. M.; Broxterman, Q. B.; Kamphuis, J. *Chem. Eur. J.* **1996**, *2*, 1104−1111.

(22) Carpino, L. A.; Mansour, E. S. M. E.; Sadat-Aalaee, D. *J. Org. Chem.* **1991**, *56*, 2611−2614.

(23) Carpino, L. A. *J. Am. Chem. Soc.* **1993**, *115*, 4397−4398.

(24) Jeener, J.; Meier, B. H.; Bachmann, P.; Ernst, R. R. *J. Chem. Phys.* **1979**, *71*, 4546−4553.

(25) Piantini, U.; Sorensen, O. W.; Bodenhausen, G.; Wagner, G.; Ernst, R. R.; Wüthrich, K. *Biochem. Biophys. Res. Commun.* **1983**, *117*, 458−479.

(26) Braunschweiler, L.; Ernst, R. R. *J. Magn. Reson.* **1983**, *53*, 521−528.

(27) Levitt, M. H.; Freeman, R. *J. Magn. Reson.* **1981**, *43*, 502−507.

function shifted by $\pi/2$ in F1 and F2 was used for apodization. The HMQC[28] and HMBC[29] (with a low-pass J filter[30]) experiments were recorded with 16 and 64 scans, respectively, and sweep widths of 22 727.27 Hz in F1 and 6009.62 Hz in F2. The digital resolution was 512 data points in F1 and 1024 in F2. The acquisition time was 85.2 ms and the relaxation delay 1.0 s. For the data processing F1 was zero-filled to 1024 real data points, and a complex linear prediction was performed using 16 coefficients. F2 was zero-filled to 4096 data points. Baseline correction was subsequently applied in both dimensions, and a squared sine bell function shifted by $\pi/2$ was used for apodization.

Spin–Echo Diffusion Measurements. Temperature-dependent spin–echo diffusion measurements were performed in the range of 273–300 K within six steps using a double stimulated echo experiment with suppression of convection artifacts.[31,32] At each temperature 75 ^{1}H spectra were recorded using square gradients and a gradient ramp between 2 and 75 G/cm with 64 scans, a sweep width of 6009.62 Hz, and a digital resolution of 16 384 real data points. The acquisition time was 1.36 s, and the relaxation delay was 5.0 s. The data were stored as a pseudo-2D experiment. The dephasing and refocusing gradient length *LD* was set to 4 ms, and the diffusion delay *BD* was 50 ms. The evaluation of the data was carried out using the T_1/T_2 relaxation menu of XWinNMR 2.6 with the provided fitting function for variable gradient strength. At each temperature 20 convergent signal decays were averaged, and a nonlinear curve fitting procedure was performed. The diffusion constants (m^2/s) at each temperature are as follow: 273 K, $2.11 \times 10^{-10} \pm 8.3 \times 10^{-12}$; 280 K, $2.53 \times 10^{-10} \pm 5.6 \times 10^{-12}$; 285 K, $2.78 \times 10^{-10} \pm 3.5 \times 10^{-12}$; 290 K, $3.17 \times 10^{-10} \pm 8.1 \times 10^{-12}$; 295 K, $3.56 \times 10^{-10} \pm 1.4 \times 10^{-12}$; 300 K, $3.93 \times 10^{-10} \pm 1.5 \times 10^{-12}$.

Simulated Annealing and Molecular Dynamics. A set of 86 interproton distances was determined from a quantitative evaluation of the NOESY spectrum. Nineteen of these were ambiguous and with a high intermolecular component, 35 were intraresidual ($i \rightarrow i$), 26 sequential ($i \rightarrow i + 1$), and 25 long range ($i \rightarrow i + n$, $n > 1$). For the calibration of the cross-peak intensity, the diastereotopic H$^\beta$ protons of (αMe)Phe^5 could not be used due to overlap. Therefore, three conformationally independent interproton distances were used and afterwards checked for consistency. The distance of the amide proton of the NHMe C-terminal blocking group to its methyl group protons was set to 2.67 Å, and the NOE intensities of Val^{2}Hβ and (αMe)-Val^{4}Hβ to their Hγ protons were set to 2.67 Å. The upper and lower limits of the distance restraints were generated after averaging cross-peak volumes on both sides of the diagonal and by adding and subtracting 10% of the NOE distance. As distances were averaged using the r^{-6} sum function[33] for ambiguous intra- and intermolecular NOEs, no pseudoatom corrections were used.

Simulated annealing (SA) calculations were performed with the X-PLOR[34] program using the *parallhdg* force field. The SA started with a random conformation of the monomeric peptide backbone. A total of 32 ps of high-temperature dynamics at 1000 K (random velocity initialization according to the Boltzmann distribution) was performed on this structure in vacuo. The temperature was decremented in 20 K steps to a value of 60 K. A final 30 ps dynamics run and a 1000 step minimization were then performed. Because of CHCl$_3$, the dielectric constant was set 4.8. An ensemble of 100 monomeric structures was generated, yielding also a partial diastereotopic assignment. For the calculation of the dimeric structure, all ambiguous intermolecular NOEs were included, and the same simulated annealing protocol was used. As starting structure, a dimeric model consistent with the intermolecular NOEs was built manually from the lowest-energy monomeric structure. Because of the singular single set which was observed in the spectra, noncrystallographic symmetry restraints (NCS)[34] were applied. Alto-

(28) Hurd, R. E.; John, B. K. *J. Magn. Reson.* **1991**, *91*, 648–653.

(29) Bax, A.; Summers, M. F. *J. Am. Chem. Soc.* **1986**, *108*, 2093–2094.

(30) Kogler, H.; Sørensen, O. W.; Bodenhausen, G.; Ernst, R. R. *J. Magn. Reson.* **1983**, *55*, 157–163.

(31) Jerschow, A.; Müller, N. *J. Magn. Reson.* **1997**, *125*, 372–375.

(32) Jerschow, A.; Müller, N. *J. Magn. Reson.* **1998**, *132*, 13–18.

(33) Nilges, M. *Proteins: Struct., Funct. Genet.* **1993**, *17*, 297–309.

(34) Brünger, A. T. *X-PLOR Version 3.1, A System for X-ray Crystallography and NMR*; Yale University Press: New Haven, 1992.
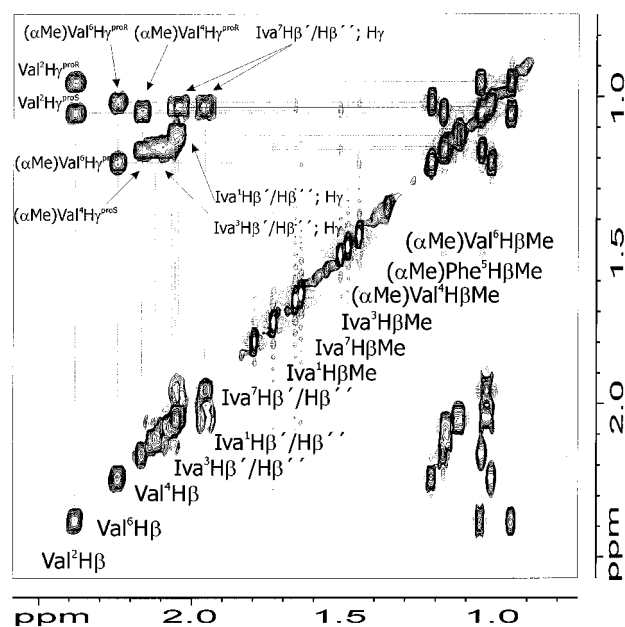
Figure 2. TOCSY spectrum of the aliphatic region of the heptapeptide, acquired with a mixing time of $\tau = 80$ ms. Despite several overlaps, a complete ^{1}H assignment could be accomplished, as indicated by the cross-peak labels.

gether, 100 dimeric structures were calculated, and the 10 structures with the lowest total energy were checked for convergence (mean backbone RMSD = 0.12 Å) and NOE distance violations. Out of 86 NOE distance restraints, 9 were violated between 0.2 and 0.4 Å. The structure with the lowest NOE distance violations was chosen for further molecular dynamics (MD) simulations in explicit CHCl$_3$.

A free MD simulation, without any restraint, was performed with the MSI Discover program using the CVFF force field.[35] For this purpose the resulting dimeric SA structure was surrounded by a cubic box of CHCl$_3$ (length, 36 Å; 241 CHCl$_3$ molecules). The system was minimized using 1000 steps of steepest descent and 1000 steps of conjugate gradients minimization for the solvent and the starting structure and then heated to 273 K in seven steps. The trajectory was recorded after an equilibration time of 500 ps for 2.5 ns at this temperature using periodic boundary conditions with a cutoff radius of 13 Å.

Results and Discussion

Due to its hydrophobicity and for comparison to a previously published study,[12] the terminally blocked heptapeptide was investigated in CDCl$_3$. Furthermore, the CDCl$_3$ solution mimicks the natural environment of a lipophilic peptide, e.g., in a membrane core.[8] All NMR measurements were performed at 273 K to stabilize the proposed helical structure of the linear peptide.

Proton spin systems in C$^\alpha$-methylated α-amino acids do not yield direct coupling information between the side chains and the backbone. In addition, low signal dispersion of the numerous methyl groups complicated the signal assignment. Spin systems of the side chains, especially of Val^2 and the N- and C-terminal blocking groups, were assigned using a TOCSY[26] spectrum (Figure 2). Sequential assignment of proton and carbonyl resonances was achieved by a combination of HMQC[28] and HMBC[29] spectra via the heteronuclear CO$_{i-1}$–H^N_i cross signals. The procedure is illustrated in Figure 3, where a superposition of the HMQC and HMBC spectra is shown, and the results are listed in Tables 1 and 2. Diastereotopic assignment of the

(35) Dauber-Osguthorpe, P.; Roberts, V. A.; Osguthorpe, D. J.; Wolff, J.; Genest, M.; Hagler, A. T. *Proteins: Struct., Funct. Genet.* **1988**, *4*, 31–47.
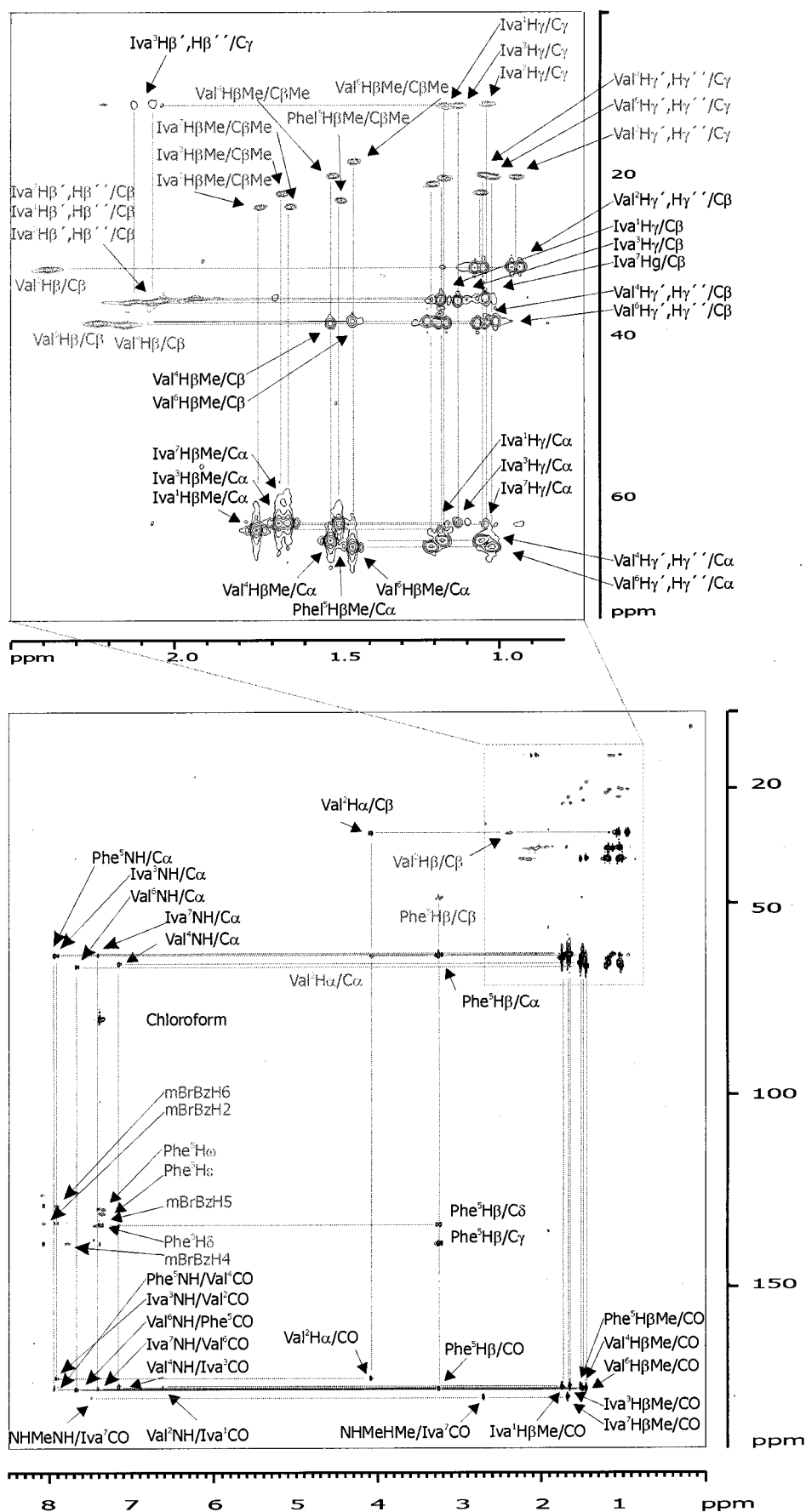
Figure 3. Superposition of an HMQC (gray) and an HMBC (black) spectrum ($\Delta = 80$ ms) to show the procedure used for sequential assignment of the heptapeptide. The upper part is an expansion of the section of the spectrum indicated in the lower part.

Table 1. ^{1}H NMR Resonances and Diastereotopic Assignment of *m*BrBz-Iva^1-Val^2-Iva^3-(αMe)Val^4-(αMe)Phe^5-(αMe)Val^6-Iva^7-NHMe at 273 K in CDCl$_3$ [ppm]

*m*BrBz		Iva^1	Val^2	Iva^3	(αMe)Val^4	(αMe)Phe^5	(αMe)Val^6	Iva^7	NHMe
H2 8.10	NH	7.37	6.72	7.91	7.15	7.94	7.67	7.41	NH 7.45
H4 7.77	Hα	-	4.07	-	-	-	-	-	HMe 2.68
H5 7.43	HβMe	1.74	-	1.64	1.52	1.48	1.45	1.67	-
H6 7.95	Hβ^l	2.05		2.11 proS		3.27		1.93 proR	-
	Hβ^h	2.05	2.38	2.06 proR	2.15	3.23	2.24	2.03 proS	
-	Hγ^l		1.05 proS	1.13	1.17 proS	-	1.21 proS		-
	Hγ^h	1.18	0.95 proR		1.05 proR		1.02 proR	1.03	
-	Hδ	-	-	-	-	7.39	-	-	-
-	Hε	-	-	-	-	7.36	-	-	-
-	Hω	-	-	-	-	7.35	-	-	-

Table 2. ^{13}C NMR Resonances of *m*BrBz-Iva^1-Val^2-Iva^3-(αMe)Val^4-(αMe)Phe^5-(αMe)Val^6-Iva^7-NHMe at 273 K in CDCl$_3$ [ppm]

*m*BrBz		Iva^1	Val^2	Iva^3	(αMe)Val^4	(αMe)Phe^5	(αMe)Val^6	Iva^7	NHMe
	CO	176.2	173.8	175.8	176.4	176.6	176.5	178.9	
C1	Cα	64.2	63.5	63.3	65.5	63.4	66.3	63.3	CMe 29.2
C2 133.1	Cβ Me	24.0	-	24.0	20.0	23.2	18.3	22.3	-
C3 125.7	Cβ	35.5	31.7	35.7	38.6	48.5	38.3	35.3	-
C4 138.5	Cγ^l	11.3	20.2	11.4	19.9	138.5	20.1	11.2	-
	Cγ^h		20.2		20.4		21.1		
C5 133.7	Cδ	-	-	-	-	133.6	-	-	-
C6 128.5	Cε	-	-	-	-	130.7	-	-	-
	Cω	-	-	-	-	129.5	-	-	-

```
            0   1   2 Hα  3   4   5   6   7   8

HN^i / HN^{i+1}        ■   ■   ■   ■   ■   ■   □

HN^i / HN^{i+2}                        ─

HN^i / HN^{i+3}

HβMe^i / HN^i     ─   ■   ■   ■   ■   ■   □         ■  < 250 pm

HβMe^{i+1} / HN^i     ─   ─   ─   ─   ─   ─         ▬  < 300 pm

HβMe^{i+2} / HN^i        ──  ──                     ─  < 400 pm

HβMe^{i+3} / HN^i          ────  ────               ─  < 450 pm

                                                   ─  < 550 pm
                                                   □  Overlap
```

Figure 4. Summary of the NOE-derived backbone distances for the heptapeptide. The width of the bars indicates the NOE intensity. Residue numbers 0 and 8 are used for the N-terminal and C-terminal blocking groups, respectively. For the restrained MD calculations, measured distances (with 10% errors) are used instead of distance classes.

γ-methyl groups of Val^2 and (αMe)Val^{4,6} residues and the β-protons of Iva^3 and Iva^7 was possible on the basis of local geometries using NOE-derived distances after the first converged simulated annealing calculations. The β-protons of Iva^1 were degenerate, and the β-protons of (αMe)Phe^5 were highly overlapped.

Strong sequential H^N_i–H$^N_{i+1}$ NOE cross-peaks confirm the helical conformation of the heptapeptide (Figure 4). Additionally, the NOESY spectrum showed a few *inter*molecular NOEs, especially from the amide proton of Val^2 to the C-terminal blocking group NHMe and from side chain to side chain, which indicate an antiparallel side-by-side aggregation or a head-to-tail aggregation, as described in the crystal structure of Boc-Val-Ala-Leu-Aib-Val-Ala-Leu-(Val-Ala-Leu-Aib)$_2$-OMe (Boc, *tert*-butyloxycarbonyl; OMe, methoxy).[36]

To corroborate the aggregation phenomenon with an additional experiment, temperature-dependent diffusion measure-

ments of the heptapeptide were performed. The diffusion coefficients were calculated by applying a fitting procedure to the signal decay (Figure 5). The calculated self-diffusion coefficient of CHCl$_3$ was used as an internal standard.[37] To estimate the hydrodynamic radius of the heptapeptide in a saturated CHCl$_3$ solution, the Stokes−Einstein equation was used by taking into account the temperature dependency of the dynamic viscosity of CHCl$_3$ and a friction factor for the helical shape $f/f_0 = 1.04$.[38] Assuming a helical geometry for the heptapeptide, as indicated by the NOESY spectrum, the hydrodynamic diameter of the monomeric helix is 15.5 Å. For an antiparallel side-by-side aggregation the hydrodynamic diameter should be about 1.5 times larger. Although the accuracy of the applied method is not very high, the calculated factors between 2.3 ± 0.1 at 273 K and 1.8 ± 0.1 at 300 K clearly indicate a dimerization.

On the basis of this information, the NOE assignments had to be carefully reinterpreted in terms of dimerization. Especially protons near the middle of the interface between the two monomers have a highly mixed intra-/intermolecular origin. This fact and the additional low signal dispersion made the assignment of the NOE cross signals more ambiguous. However, these ambiguities were checked after every SA calculation and, if possible, cleared during the refinement of the structure. During the first structure calculation, all NOE distance restraints which were recognized as obviously intermolecular were excluded, and only the monomeric structure was considered. To prevent bias, several randomly generated conformations of the linear peptide were used as starting structures. One NOE, (αMe)Phe^{5}Hβ′/″−(αMe)Phe^{5}Hε′/″, was significantly violated in all SA runs. The distance restraint given by that NOE was 0.5 Å shorter than the minimum geometrically possible distance. This provided evidence for an antiparallel side-by-side aggregation in which the two phenyl rings of Phe^5 in the two monomers are in close contact. Thus, a dimeric starting structure was generated out of the first helical monomeric structures which was consistent with these data, and all ambiguous intermolecular NOEs were included during the next SA calculations (Figure 6). The 10 structures with the lowest total energy converged to a backbone RMSD of 0.12 Å, and the dimeric structure with the lowest NOE distance restraint energy was chosen for further analysis. Nine distance restraints were violated by 0.2−0.4 Å, partly due to side chain flexibility of Val^2 (with a predominating trans conformation) and Iva^3 [with a predominating *gauche*(−) conformation]. The dimeric structure calculation also resulted in a refined monomeric helix, which could be classified according to the Kabsch−Sander algorithm[39] as an α-helix from Val^2 to Iva^7. A stereoplot of the monomeric heptapeptide structure is given in Figure 7. Conformational parameters such as the backbone torsion angles ϕ, ψ or the interproton distances are close for the α- and the 3_{10}-helices. There are only a few NOE distances which discriminate between these two helical conformations: for α- and 3_{10}-helices $d_{\alpha N}(i, i+2)$ should be 4.4 and 3.8 Å, respectively, while $d_{\alpha H\beta}(i, i+3)$ varies between 2.5 and 4.4 Å and between 3.1 and 5.1 Å, respectively.[40,41] The NOE distance $d_{\alpha N}(i, i+4)$ is above 4 Å in both helical conformations and thus gives rise to very weak intensity. However, the complete absence of this NOE might indicate a

(36) Karle, I. L. *Acta Crystallogr.* **1992**, *B48*, 341−356.

(37) *CRC Handbook of Chemistry and Physics*; CRC Press: Cleveland, 1998.

(38) Holde, K. E. V. *Physical Biochemistry*; Prentice Hall: Englewood Cliffs, NJ, 1998.

(39) Kabsch, W.; Sander, C. *Biopolymers* **1983**, *22*, 2577−2637.

(40) Wüthrich, K. *NMR of Proteins and Nucleic Acids*; Wiley: New York, 1986.

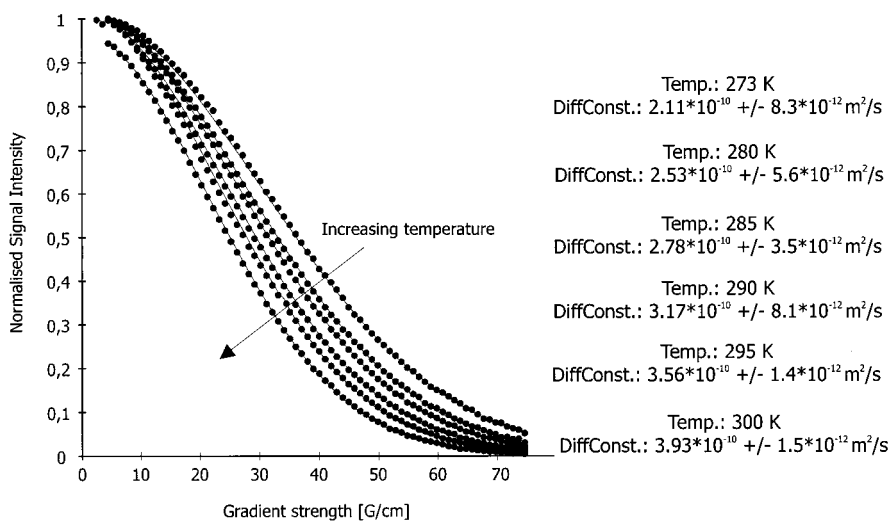(41) Wüthrich, K. *Science* **1989**, *243*, 45−50.

Figure 5. Temperature-dependent signal decay of the heptapeptide using a pulsed-field gradient echo diffusion experiment. The data were acquired at temperatures of 273, 280, 285, 290, 295, and 300 K (from right to left).
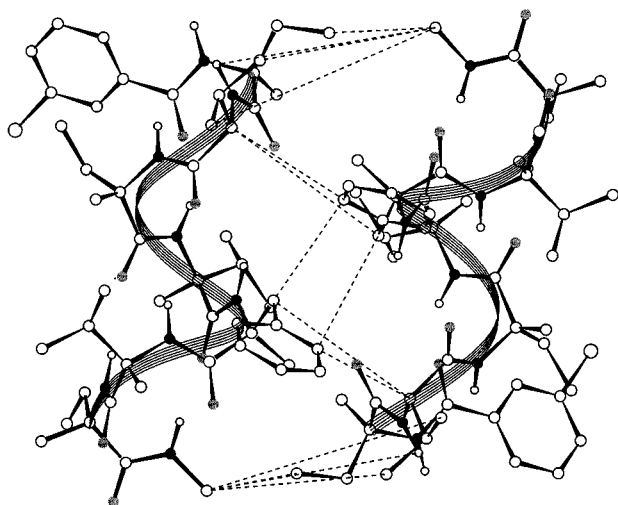

Figure 6. Relative orientation of the two monomers within the dimeric complex. NOE distance restraints with a high intermolecular share define the antiparallel side-by-side aggregation of the heptapeptide (broken lines).

Table 3. Characteristic Distances (pm) for an Ideal Model α-Helix and an Ideal Model 3_{10}-Helix in Comparison to the Experimental Peptide Helix of mBrBz-Iva[1]-Val[2]-Iva[3]-(αMe)Val[4]-(αMe)Phe[5]-(αMe)Val[6]-Iva[7]-NHMe[a]

H$^\alpha$H^N($i, i + 2$) [pm]	α helix	expt. helix	3_{10} helix
Iva[1]C$^\beta$Me – Iva[3]H^N	485	479	442
Val[2]H$^\alpha$ – (αMe)Val[4]H^N	447	426	396
Iva[3]C$^\beta$Me – (αMe)Phe[5]H^N	474	433	418
(αMe)Val[4]C$^\beta$Me – (αMe)Val[6]H^N	476	442	420
(αMe)Phe[5]C$^\beta$Me – Iva[7]H^N	470	493	413
(αMe)Val[6]C$^\beta$Me – NHMeHN	447	457	431
H$^\alpha$H^N($i, i + 4$) [pm]			
Iva[1]C$^\beta$Me – (αMe)Phe[5]H^N	437	573	584
Val[2]H$^\alpha$ – (αMe)Val[6]H^N	447	578	586
Iva[3]C$^\beta$Me – Iva[7]H^N	453	534	597
(αMe)Val[4]C$^\beta$Me – NHMeHN	479	445	590
C'C'($i, i + 3$) [pm]			
mBrBzCO – Iva[3]CO	457	457	489
Iva[1]CO – (αMe)Val[4]CO	499	569	551
Val[2]CO – (αMe)Phe[5]CO	512	565	563
Iva[3]CO – (αMe)Val[6]CO	516	544	568
(αMe)Val[4]CO – Iva[7]CO	506	486	552
H$^\alpha$H$^\beta$($i, i + 3$) [pm]			
Iva[1]C$^\beta$Me – Iva[3]H$^{\beta'/''}$	276	355	380
Val[2]H$^\alpha$ – (αMe)Val[4]H$^{\beta'/''}$	355	372	398
Iva[3]C$^\beta$Me – (αMe)Phe[5]H$^{\beta'/''}$	273	381	412
(αMe)Val[4]C$^\beta$Me – Iva[7]H$^{\beta'/''}$	276	271	357

[a] The preferred helix type in the peptide is marked in gray.

3_{10}-helical population due to its more elongated geometry. Hence, an unambiguous identification of populations of each helix type by NMR methods in solution is severely limited, unless [15]N- and carbonyl ^{13}C-labeled samples would allow the direct measurement of intramolecular hydrogen-bonding donors and acceptor atoms and their populations.[42−44] With the exception of Val[2], the heptapeptide lacks all H$^\alpha$ protons which are essential for conformational analysis on the basis of the above-mentioned characteristic NOEs. Furthermore, basing the structure of the whole peptide on the presence and relative intensity[45] of one or two NOEs involving one residue only (Val[2]) seemed unjustified. However, a detailed analysis of the resulting structure using all experimental data, in particular typical distances, torsion angles, and hydrogen bond patterns, provides evidence that the peptide rather adopts an averaged structure in a $3_{10}/\alpha$-helical equilibrium fast on the NMR time scale (100 ms mixing time in the NOESY experiment) without a clear

preference for one of the helix types (Table 3). The peptide backbone RMSD is 0.61 Å away from an ideal α-helix model and 0.57 Å from an ideal 3_{10}-helix model (the backbone RMSD between an ideal α-helix and an ideal 3_{10}-helix is 0.83 Å). Thus, compared to the fully C$^\alpha$-methylated heptapeptide analogue, which adopts predominantly a 3_{10}-helix,[12] the present heptapeptide with the missing C$^\alpha$-methylation of Val[2] is more likely to show a $3_{10}/\alpha$-helical equilibrium with a slight preference for the α-helical conformation.

The calculated dimer structure is shown in Figure 8 as a space-filling Connolly surface of each monomer and is held together by favorable lipophilic interactions. Karle[36] has shown, by X-ray diffraction structures of helical peptides, that the dominating factor of packing motifs in apolar helices is not their dipolar nature but rather a shape selection, such as a bulge fitting into a groove.[36] Thus, shape complementarity is essential for molecular recognition of the apolar helices. This property is fulfilled by our model peptide. The bulge, which enables a fitting of the helices, is mainly caused by the phenyl rings of the Phe[5] residues. The tilt angle between the helices was measured using Molmol 2.6[46] as 165°, so that the antiparallel helices are twisted by 15°.

(42) Dingley, A. J.; Grzesiek, S. *J. Am. Chem. Soc.* **1998**, *120*, 8293−8297.

(43) Cordier, F.; Grzesiek, S. *J. Am. Chem. Soc.* **1999**, *121*, 1601−1602.

(44) Gemmecker, G. *Angew. Chem.* **2000**, *112*, 1276−1279.

(45) Millhauser, G. L.; Stenland, C. J.; Hanson, P.; Bolin, K. A.; van de Ven, F. J. M. *J. Mol. Biol.* **1997**, *267*, 963−974.
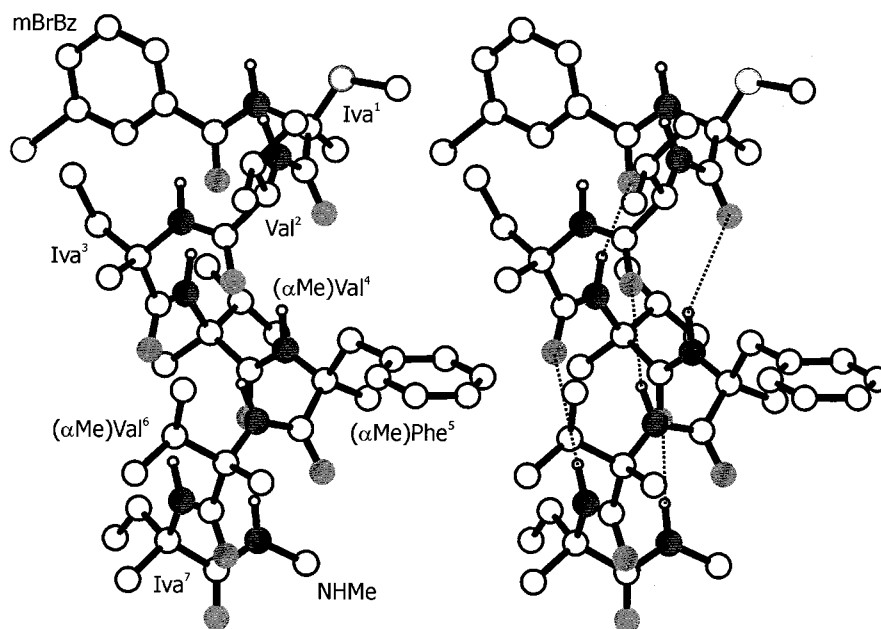
Figure 7. Stereoplot of the monomeric heptapeptide structure. Dotted lines represent hydrogen bonds.
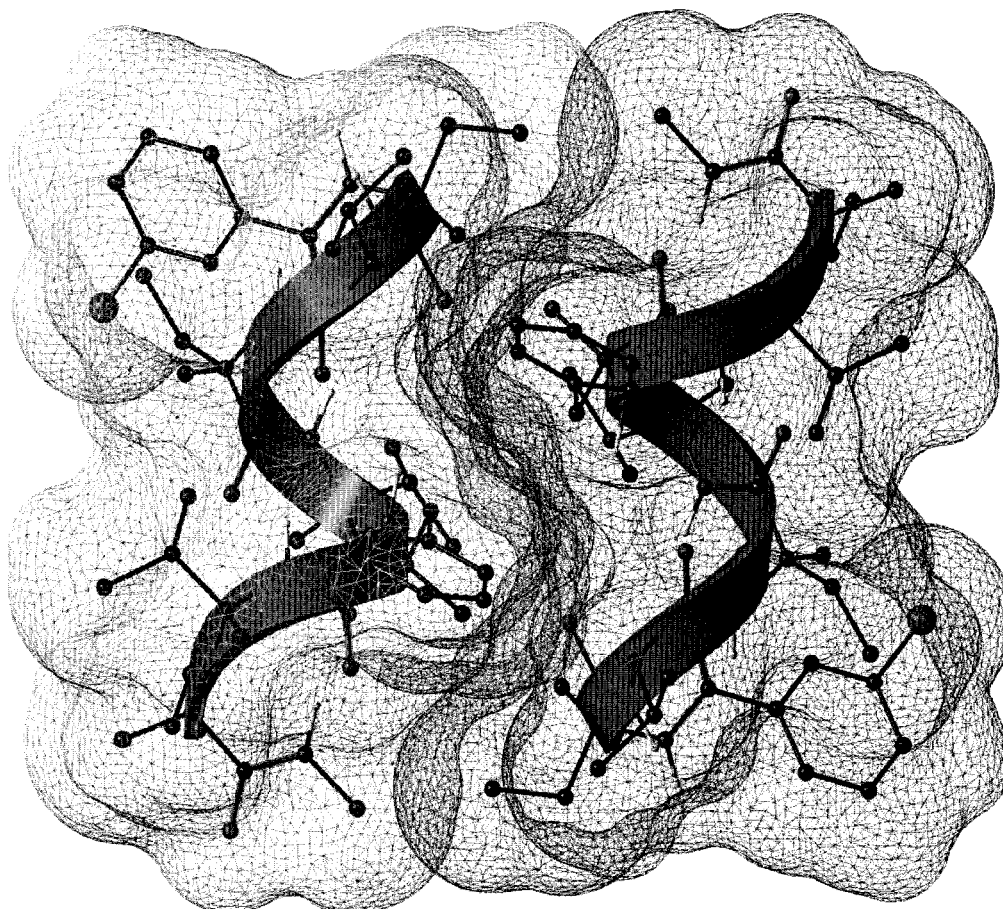

Figure 8. Dimeric structure of the heptapeptide showing the antiparallel side-by-side aggregation in the sense of a bulge fitting into a groove using a van der Waals surface.

It has been shown[47-49] that helices are flexible on the nanosecond to picosecond time scale and undergo transitions among 3_{10}-helical, α-helical, and random coil conformations.

For this reason and to show the stability of the dimeric structure, a free molecular dynamic simulation over 3 ns without any NOE distance restraint was performed in a cubic box of $CHCl_3$ at 273 K. Figure 9 shows the trajectory after an equilibration time

(46) Koradi, R.; Billeter, M.; Wüthrich, K. *J. Mol. Graphics* **1996**, *14*, 51−55.

(47) Orekhov, V. Y.; Korzhnev, D. M.; Diercks, T.; Kessler, H.; Arseniev, A. S. *J. Biomol. NMR* **1999**, *14*, 345−356.

(48) Huston, S. E.; Marshall, G. R. *Biopolymers* **1994**, *34*, 75−90.

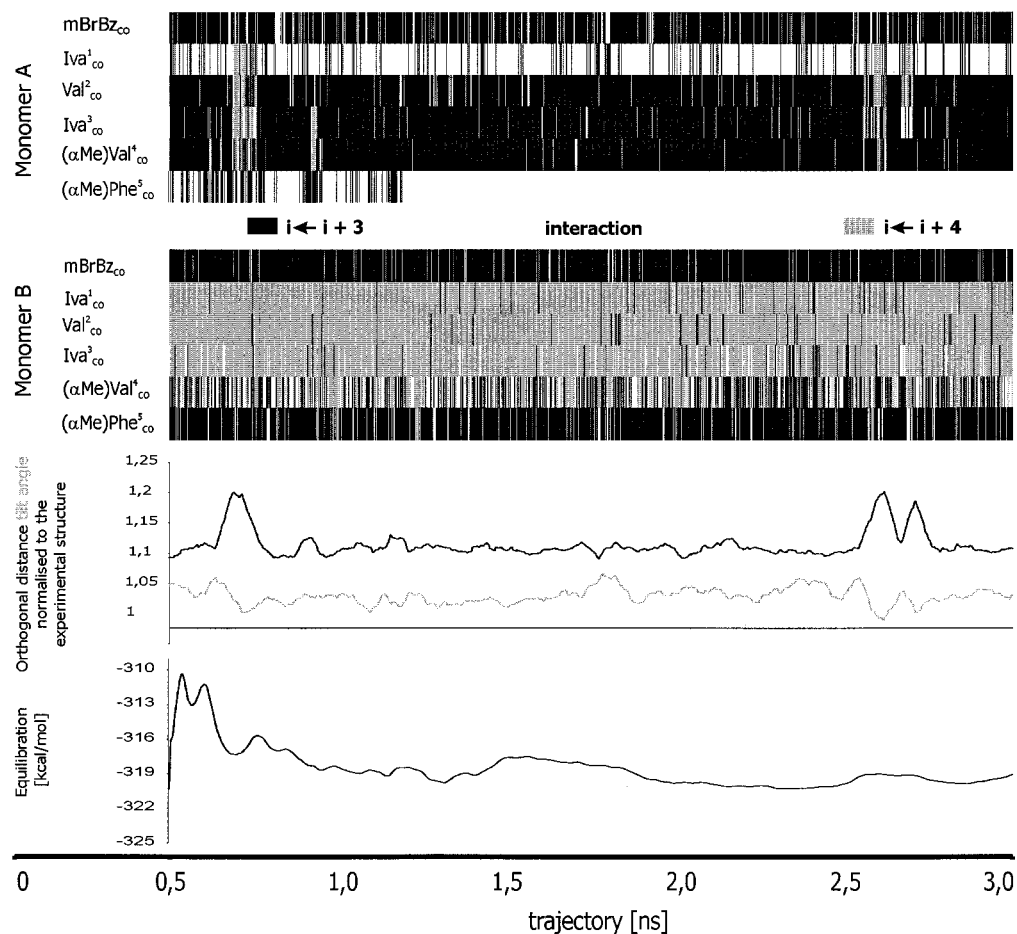(49) Tirado-Rives, J.; Maxwell, D. S.; Jorgensen, W. L. *J. Am. Chem. Soc.* **1993**, *115*, 11590−11593.

Figure 9. Free molecular dynamics simulation of the dimeric structure of the heptapeptide in a cubic box of $CHCl_3$ over 3 ns using periodic boundary conditions. (1) Hydrogen bonding pattern for each monomer: α-helical (gray bars) and 3_{10}-helical (black bars) hydrogen bonds are indicated for each residue. A hydrogen bond CO···HN is indicated if the O···H distance is shorter than or equivalent to 2.80 Å and the C−O···HN− and CO···H−N angles are larger than 110°. (2) Orthogonal distance (black) and tilt angle (gray) between the monomers normalized to the experimental structure. (3) Trajectory after an equilibration time of 500 ps. The time-averaged potential energy of the system is given in kilocalories per mole.

of 500 ps. Monitored are the hydrogen bond populations for 3_{10}-helical $i \leftarrow i + 3$ and α-helical $i \leftarrow i + 4$ interactions for each residue in either monomer. A CO···HN hydrogen bond is indicated for an O···H distance shorter than or equivalent to 2.8 Å and if the C−O···HN− and CO···H−N angles exceed 110°. Further, the diagram shows the orthogonal distance and the tilt angle between the two helices, which are normalized to the experimentally determined structure. The time-averaged potential energy of the system is given in kilocalories per mole. During the trajectory, monomer A is predominantly 3_{10}-helical, whereas monomer B is more α-helical, with the exception of the N- and C-termini adopting an $i \leftarrow i + 3$ interaction. Analyzing the backbone torsion angles ϕ,ψ,[50] it turns out that these $i \leftarrow i + 3$ interactions are either β-III turns[51] with $\phi_i = -60°$ and $\psi_i = -30°$, consistent with a 3_{10}-helix,[14,15] or at the N-terminus a β-II′ turn with $\phi_{i+1} = +60°$ and $\psi_{i+1} = -120°$ and $\phi_{i+2} = -80°$ and $\psi_{i+2} = 0°$. Furthermore, the simulation showed transitions of monomer A from a 3_{10}-helical to an α-helical conformation and vice versa of the residues Iva¹, Val², Iva³, and (αMe)Val⁴. These transitions occur in approximately 30 ps. As a consequence, the orthogonal distance between the two monomers increases when both adopt a more α-helical conformation, which is broader than a 3_{10}-helical conformation.

The tilt angle stays more or less constant over the trajectory and agrees with the angle derived from the SA strategy. Only a very small reorganization of the tilt angle is seen upon helical transitions. Two α-helical conformations occur simultaneously only for a short time of approximately 150 ps, and then the system returns to a mixed 3_{10}/α-helical conformation of the monomers while the dimeric structure stays stable over the whole 3 ns. This finding suggests that, in terms of a stable aggregation, the conformation with two pure α-helices is unfavorable, which is in agreement with the vibrational and electronic CD data of the related Z-[L-(αMe)Val]₈-O*t*Bu (O*t*Bu, *tert*-butoxy) homopeptide. These spectroscopic results indicated a stabilization of the 3_{10}-helical conformation at high concentrations upon self-aggregation; however, at low concentrations the octamer showed a propensity for a mixed 3_{10}/α-helical structure.[52]

Conclusions

NMR spectroscopy was used to characterize the 3D structure of a linear, highly C$^\alpha$-methylated, N- and C-blocked heptapeptide in CDCl₃ solution. Strong sequential H^N−H^N NOEs indicate a helical conformation. Additionally, both intermolecular NOEs

(50) IUPAC−IUB Commission on Biochemical Nomenclature. *Biochemistry* **1970**, *9*, 3471−3479.

(51) Venkatachalam, C. M. *Biopolymers* **1968**, *6*, 1425−1436.

(52) Yoder, G.; Polese, A.; Silva, R. A. G. D.; Formaggio, F.; Crisma, M.; Broxterman, Q. B.; Kamphuis, J.; Toniolo, C.; Keiderling, T. A. *J. Am. Chem. Soc.* **1997**, *119*, 10278−10285.

and NOEs with a high intermolecular component suggest an antiparallel side-by-side aggregation. Temperature-dependent calculations of the hydrodynamic radius from diffusion measurements, which correspond to an oligomer of an at least dimeric order, corroborated these findings. For the structure calculation a simulated annealing strategy was used, initially considering only the monomeric structure by excluding all NOEs which were recognized as intermolecular. During the refinement of the structure, all intermolecular and ambiguous NOEs were included, starting now from a consistent dimeric structure model. Structural calculations resulted in an antiparallel aggregated structure of two right-handed helical monomers with a slight preference for an α-helical conformation.

Discrimination between predominant 3_{10}-helix or α-helix by NMR spectroscopy is difficult. Only very few NOEs, like $d_{\alpha N}$-$(i,i+2)$, show slight differences, but there is no unique characteristic NOE which unambiguously discriminates between these two helical conformations. In addition, one has to keep in mind that transitions between either helix type and random coil may take place in solution on a time scale of pico- to nanoseconds. Thus, on the NMR time scale of milliseconds (100 ms mixing time in the NOESY experiment), both conformations are populated. As, with the exception of Val[2], the heptapeptide lacks all H^{α} protons necessary for a reasonable estimation of relative populations, all available experimental data were used, leading to a population-averaged structure. However, a detailed analysis of the structure showed that some characteristic distances, torsion angles, and hydrogen bonds are in favor of an α-helix, while others favor a 3_{10}-helix. The heptapeptide investigated in this work is an analogue of mBrBz-Iva[1]-(α*Me*)*Val*[2]-Iva[3]-(αMe)Val[4]-(αMe)Phe[5]-(αMe)Val[6]-Iva[7]-NHMe, which we found previously[12] to adopt an almost pure 3_{10}-helix form in CDCl₃ solution. This latter heptapeptide is *completely* based

on C^{α}-methylated amino acids and is thus conformationally more constrained. The missing C^{α}-methylation of Val[2] in the present heptapeptide seems to introduce some flexibility, which has an impact on its overall structure. An unrestrained molecular dynamics simulation of the dimeric helices in CDCl₃ solution over 3 ns showed that both the helical secondary structure and the antiparallel dimeric structure are stable. Furthermore, transitions between the two helical conformations are seen on a time scale of picoseconds, but the most populated hydrogen bonds are those typical of a 3_{10}-helix in monomer A and of an α-helical in monomer B. The dimeric structure is held together by favorable van der Waals interactions in the sense of a bulge fitting into a groove. The native-like environment for a lipophilic peptide is mimicked by the CHCl₃ solution. Thus, the heptapeptide studied here is a good model in which two relevant aspects of trans-membrane protein folding are present according to the two-stage model[1] (or, in the case of globular proteins, according to the diffusion−collision model[53]). First, flexible $i \leftarrow i + 4$ and $i \leftarrow i + 3$ hydrogen bonds build up a stable local structure, which is responsible for the onset of a specific molecular shape. Second, this shape is recognized as attractive by other surrounding structures via electrostatic forces and lipophilic interactions in combination with a complementary shape.

(53) Karplus, M.; Weaver, D. L. *Nature* **1976**, *260*, 404−406.